eXPRESS Polymer Letters Vol.9, No.8 (2015) 736–743
Available online at www.expresspolymlett.com
DOI: 10.3144/expresspolymlett.2015.68

Fabrication of polyaniline coated iron oxide hybrid particles and their dual stimuli-response under electric and magnetic fields

*B. Sim, H. S. Chae, H. J. Choi**

Department of Polymer Science and Engineering, Inha University, 402-751 Incheon, Korea

Received 13 January 2015; accepted in revised form 9 March 2015

Abstract. Polyaniline (PANI)-coated iron oxide (Fe_3O_4) sphere particles were fabricated and applied to a dual stimuli-responsive material under electric and magnetic fields, respectively. Sphere Fe_3O_4 particles were synthesized by a solvothermal process and protonated after acidification. The aniline monomer tended to surround the surface of the Fe_3O_4 core due to the electrostatic and hydrogen bond interactions. A core-shell structured product was finally formed by the oxidation polymerization of PANI on the surface of Fe_3O_4. The formation of Fe_3O_4@PANI particles was examined by scanning electron microscope and transmission electron microscope. The bond between Fe_3O_4 and PANI was confirmed by Fourier transform-infrared spectroscope and magnetic properties were analyzed by vibration sample magnetometer. A hybrid of a conducting and magnetic particle-based suspension displayed dual stimuli-response under electric and magnetic fields. The suspension exhibited typical electrorheological and magnetorheological behaviors of the shear stress, shear viscosity and dynamic yield stress, as determined using a rotational rheometer. Sedimentation stability was also compared between Fe_3O_4 and Fe_3O_4@PANI suspension.

Keywords: *smart polymers, electrorheology, magnetorheology, polyaniline, iron oxide*

1. Introduction

The reversible phase transitions as a response to external stimuli, such as pH, temperature, ionic strength, shear, electric or magnetic fields become a significant area of materials research [1–8]. Electric or magnetic stimuli-responsive suspension systems are particularly noticeable because their dramatic changes in shear viscosity and yield stress under a range of conditions is useful for rheology control applications. For example, suspensions consisting of magnetic particles dispersed in a nonmagnetic liquid have controllable properties under an external magnetic field [9]. If magnetic fields are applied to suspensions, their shear viscosity increases significantly and causes solidification. The magnetic dipole-dipole interactions are induced between the adjacent magnetic particles and fibrillar structures along the direction of the magnetic fields are formed. Therefore, a liquid-like suspension is transformed quite rapidly to a solid-like state [10]. As soon as the magnetic field is removed, the suspension returns rapidly to its original free flowing liquid state. These suspensions are called magnetorheological (MR) fluids or suspensions. The reversible magnetization and demagnetization upon the application of an eternal magnetic field applied alters the rheological properties of suspensions. Similar to MR suspensions, electrorheological (ER) fluids are composed of electrically polarizable particles dispersed in an insulating liquid and features electrically reversible and tunable behavior [11].

*Corresponding author, e-mail: hjchoi@inha.ac.kr

Soft magnetic carbonyl iron (CI) microspheres are the most popular MR materials because of their excellent magnetic behavior but their large density causes severe sedimentation problems. To overcome this drawback, iron oxide (Fe_3O_4) particles, which have lower density but sufficient magnetic properties, were adopted. Furthermore, due to their oxidation state these magnetic particles are not easily affected by the corrosion under acidic conditions compared to the CI particles [12]. Concurrently, as an electro-responsive material, polyaniline (PANI), has been investigated extensively in ER systems [13–15] because of its easy synthesis, good thermal stability, low cost, and reversible doping/dedoping process to control the conductivity. Both ER and MR fluids have been studied extensively but there are only a few reports on electrorheological/magnetorheological (EMR) suspensions. For example, EMR performance-based polypyrrole/Fe_3O_4 composites [16] and synergistic effect of EMR suspensions have been investigated [17–19].

In this study, PANI-coated Fe_3O_4 particle-based EMR suspensions were prepared. A hybrid of dielectric and magnetic particles revealed dual stimuli-responses. The ER and MR experiments were conducted respectively using a rotational rheometer.

2. Experimental

2.1. Materials and preparation

Spherical Fe_3O_4 microspheres were synthesized using a solvothermal process, in which initially 10.8 g of ferric chloride hexahydrate (Sigma-Aldrich) and 14.4 g of sodium acetate (Sigma-Aldrich) were dissolved in 200 mL of ethylene glycol (Daejung Co. Ltd., Korea) with vigorous stirring. The solution was transferred to a Teflon-lined stainless-steel autoclave, sealed and heated at 200°C for 24 h. The resulting product was washed several times with ethanol and distilled water.

And then, 1 g of Fe_3O_4 was added to a three-neck flask containing 400 mL of HCl (0.1 M, Duksan, Korea) and sonicated for 30 min using a sonication bath (Powersonic 410, 40 kHz, 500 W, Hawshin Tech., Korea) After stirring reactor for 10 h at 5°C, the solution was decanted by the application of an external magnet. Subsequently, 100 mL of anhydrous ethanol and 1 mL of aniline (DC Chemical, Korea) were added to the reactor. The solution was sonicated for 10 min and stirred slowly at 5°C in a nitrogen atmosphere. After being kept for 12 h, 1.7 mL of HCl (12 M) was added, and then 250 mL of ammonium persulfate (0.04 M, Daejung Co., Korea) was also added dropwise over a ca. 30 min period. The mixture was stirred vigorously in a nitrogen atmosphere for 8 h. Finally, the resulting product was collected magnetically and washed with ethanol and distilled water [20].

To prevent dielectric breakdown under applied high electric field strength, we dedoped the particles using 1 M NaOH solution as follows. Once the particles were dispersed in distilled water by adjusting the pH value to 7, they were washed with distilled water several times and then dried in vacuum oven. Their electrical conductivity was measured to be in a semiconducting region with $5.56 \cdot 10^{-8}$ S/cm.

The EMR suspension was prepared by dispersing the particles in insulating silicone oil (Shin-Etsu silicone, KF-96, kinematic viscosity at 25°C: 50 mPa·s, specific gravity at 25°C: 0.96 g/cm^3).

2.2. Characterization

The chemical structure of the PANI-coated Fe_3O_4 was analyzed by Fourier transform-infrared spectroscope (FT-IR) (VERTEX 80v, Bruker). KBr powder was used to make the pellet and measured by a transmission mode. The morphology and elemental composition were characterized by high resolution-scanning electron microscope (HR-SEM) (SU-8010, Hitachi) combined with an energy dispersive X-ray analyzer (EDS) (EX-250, HORIBA). The transmission electron microscope (TEM) (CM200, Philips) also used to observe core-shell structures. Thermal stability was determined by thermogravimetric analysis (TGA) (STA 409 PC, NETZSCH) heated up to 800°C at a heating rate of 10°C/min under an atmospheric condition. Magnetic properties were examined on the powder state using a vibration sample magnetometer (VSM) (Lakeshore 7307). Gas pycnometer (AccuPyc 1330, Micromeritics) was used to measure the particle density. The ER properties were examined using a rotational rheometer (MCR 300, Anton Paar) connected to a high voltage power supplier (HCN 7E-12 500, Fug) and the suspension was placed in the Couette-type geometry with a bob and cup (CC 17/E, gap distance: 0.71 mm). The MR properties were investigated using a parallel-plate (PP 20, gap distance: 1 mm) geometry equipped with a MR device (Physica MRD 180, Anton Paar). A Turbiscan lab expert system (Turbiscan Classic MA2000, Formulaction) was used to confirm the

sedimentation stability. All characterizations were conducted at room temperature.

3. Results and discussion

The FT-IR spectra confirmed the successful polymerization of aniline onto the Fe_3O_4 surface, as shown in Figure 1. In the Fe_3O_4@PANI spectrum, the peaks at approximately 3384 cm^{-1} (free N–H stretching vibration band in association with hydrogen bond), 1585 and 1498 (C=N and C=C stretching vibration of the quinoid and benzenoid ring, respectively), 1304 and 1143 (C–N stretching of the secondary aromatic amine), 1247 (C–N stretching vibration in protonic acid doped PANI), and 829 cm^{-1} (out of plane deformation of C–H in the 1,4-disubstituted benzene ring) were assigned to the characteristics of pure PANI [21, 22]. All of them were blue-shifted compared to the pure PANI peaks (1568, 1492, 1303, and 1135 cm^{-1}) because the N atoms with lone pairs of electrons in PANI are inclined to adsorb to the surface hydroxyls of Fe_3O_4 by hydrogen bonding, which decreases the electron cloud density of C=C, C=N and C–N bonds in the conjugated quinoid and/or benzenoid rings. At the same time, the characteristic peak of Fe_3O_4 at 584 cm^{-1} (Fe–O stretching) [23] shows a red-shift compared to 592 cm^{-1} for pure Fe_3O_4 due to weakening of the surface Fe–O bonds. As a result, the bond between Fe_3O_4 and PANI is a definite combination rather than just a blend of two components [24].

SEM images in Figure 2 present the morphology of particles. Pure Fe_3O_4 is spherical with a grainy surface. After the polymer coating process, the surface of the composite is changed, evidently due to the growth of PANI on the Fe_3O_4 surface. TEM images revealed well-defined core-shell structures of Fe_3O_4@PANI. After an acidifying step of the Fe_3O_4 core, the aniline monomer was adsorbed onto the Fe_3O_4 surface through electrostatic and hydrogen bonding. PANI can nucleate and grow on the Fe_3O_4 surface to form a core-shell structure. The core-shell structure can be hardly formed in the absence of protonation of the core. Without an acidifying process of Fe_3O_4, bare Fe_3O_4 particles are mainly

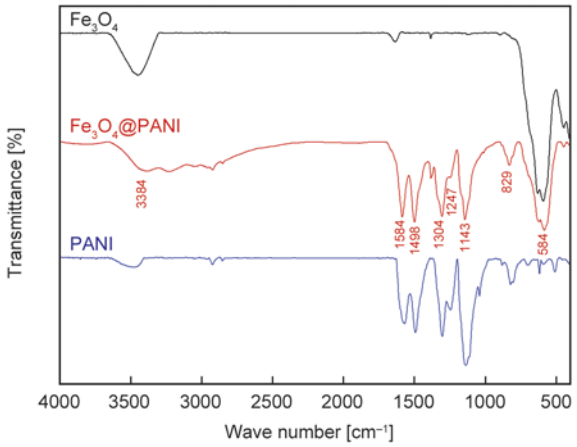

Figure 1. FT-IR spectra of Fe_3O_4, Fe_3O_4@PANI and PANI

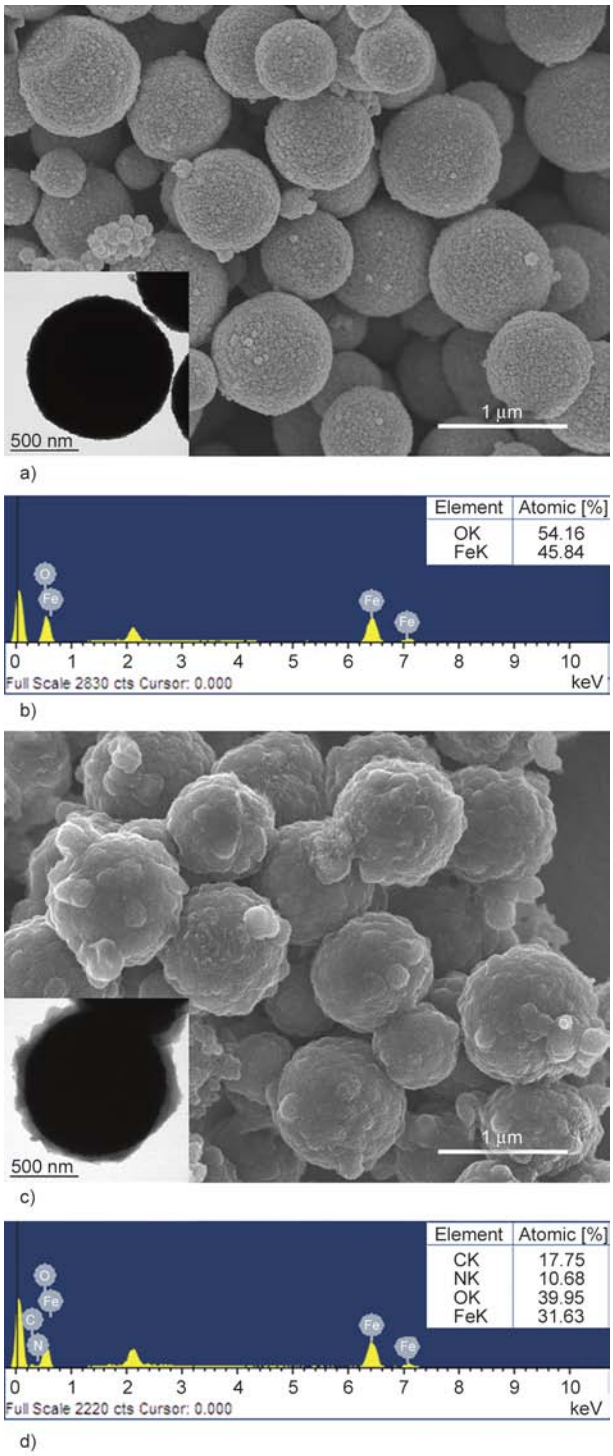

Figure 2. SEM and TEM (inset) images of (a) Fe_3O_4, (c) Fe_3O_4@PANI and EDS results of (b) Fe_3O_4, (d) Fe_3O_4@PANI (Pt from Pt coating is removed)

formed. This proves that acidification is essential for preparing the Fe_3O_4@PANI structure and those other surfactants are unnecessary [20]. Further composition was analyzed by SEM-EDS spectra. In Figure 2d, the peaks corresponding to C, N, O and Fe confirmed the presence of the PANI coating on the Fe_3O_4 surface, indicating the successful fabrication. To calculate the amount of PANI incorporated on Fe_3O_4@PANI, the thermal analysis was carried out as shown in Figure 3. The weight loss around 100°C is attributed to the release of water and dopant from the PANI. The sharp degradation of PANI observed around 350°C and continues to 600°C due to large scale thermal degradation of the PANI chains. Fe_3O_4@PANI underwent a similar decomposition behavior as like PANI, but it possessed an enhanced thermal stability with a slower rate of weight loss. It was certain that the Fe_3O_4 particles can improve the thermal stability of the composite due to an interaction between Fe3O4 and PANI chains which restricts the thermal motion [25]. The content of Fe_3O_4 in the composite was approximately 63.91 and about 33.84 wt% of PANI was coated.

Figure 4 presents magnetic hysteresis loop of Fe_3O_4 and Fe_3O_4@PANI which was measured by a VSM under a magnetic field from –10 to 10 kOe. The values of saturation magnetization, remnant magnetization and coercivity of Fe_3O_4 are 64, 2.6 emu/g and 39.5 Oe, respectively, while those of Fe_3O_4@PANI are 38, 2.2 emu/g and 39.7 Oe, respectively. The decrease in the saturation of magnetization was attributed to the introduction of non-magnetic PANI. Also, a low coercivity value demonstrated their superparamagnetism [20] which is beneficial for the reversible MR systems.

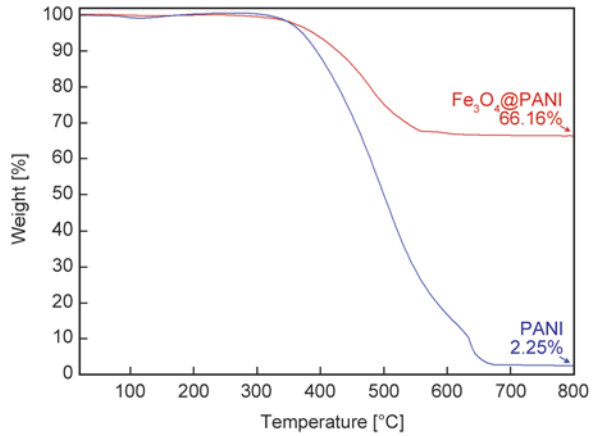

Figure 3. TGA curves of Fe_3O_4@PANI and PANI

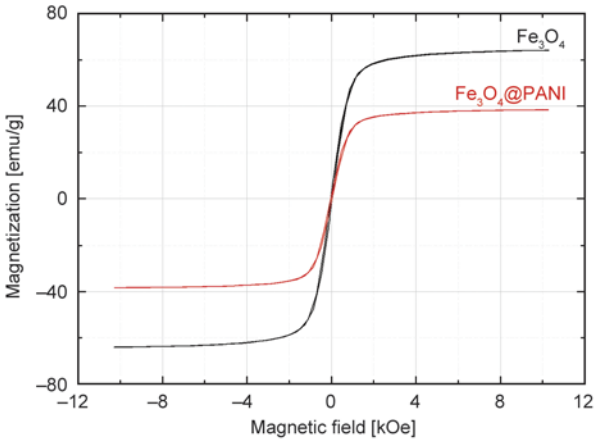

Figure 4. Magnetization curves of Fe_3O_4 and Fe_3O_4@PANI

To examine the electric responses of the suspension, the controlled shear rate mode was tested using Couette-type geometry with a rotational rheometer, as shown in Figure 5a. Typically, the suspension behaves like a Newtonian fluid in the absence of an electric field, where the shear stress increases linearly with increasing shear rate [26]. In contrast, under high electric fields, the suspension requires a certain yield stress to initiate shear flow and a shear stress to become stable at the low shear rate region. A large increase in shear stress was caused by the polarized particles and inter-particle interaction force [27]. The yield stresses of the suspension, which was estimated by extrapolating the shear stress to a zero shear rate was enhanced from 13 to 144 Pa with increasing electric field strength from 0.5 to 2.5 kV/mm.

The suspension between the parallel-plate cells was loaded to examine the magnetic responses. The shear stresses were measured as a function of the shear rate ranging from 0.1 to 500 s^{-1} under a magnetic field (Figure 5b). At a zero magnetic field, the suspension behaved like a general fluid, which shows linearity between the shear stress and shear rate. On the other hand, it acted as a Bingham fluid [28] under an external magnetic field with a yield stress due to the formed particle cluster or chains by polarization forces [29]. The yield stresses increased from 30 to 437 Pa under magnetic field strengths from 86 to 342 kA/m. As the polarization force between the particles became stronger, a more rigid chain-like structure can be formed [30]. These improved robust structures can explain why the shear stress is independent of the shear rate and why the yield stress increased with increasing magnetic field strength.

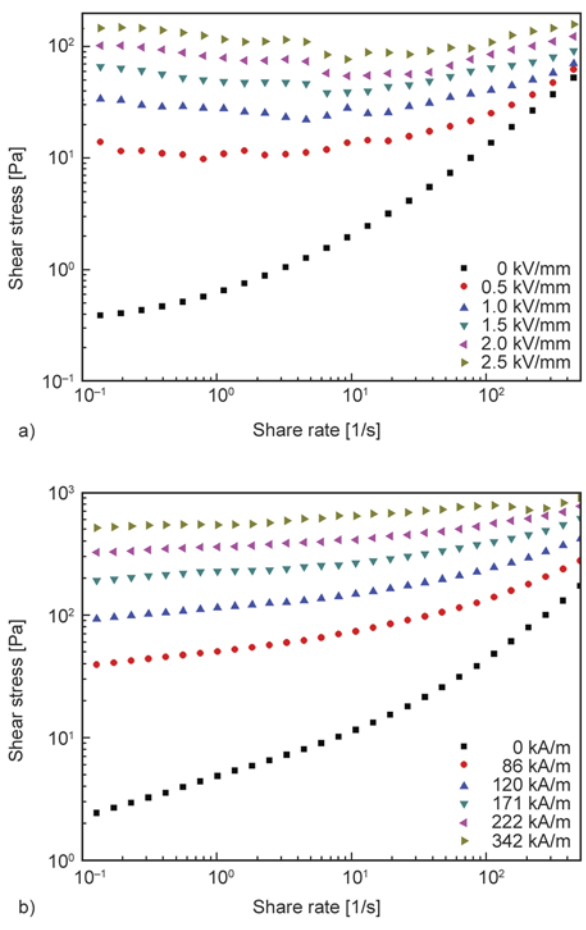

Figure 5. Flow curves of 20 wt% Fe_3O_4@PANI suspension under a) electric and b) magnetic fields

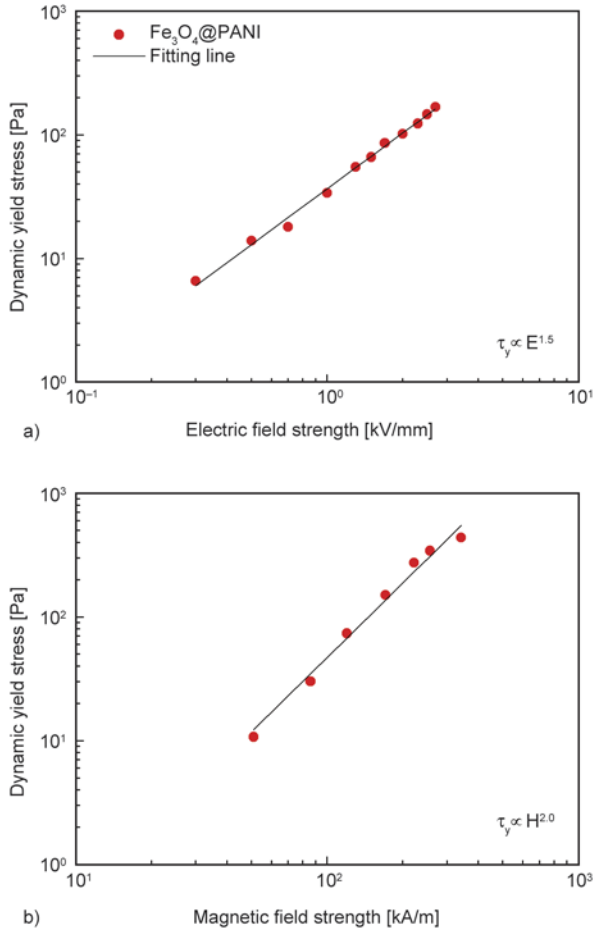

Figure 6. Dynamic yield stress of 20 wt% Fe_3O_4@PANI suspension under a) electric and b) magnetic fields

In particular, the induced magnetostatic force is larger than the hydrodynamic force between particles [31].

In Figure 6, dynamic yield stresses (τ_y) were reanalyzed as a function of electric and magnetic field strengths from Figure 5 by extrapolating shear stress to zero shear rate. In the presence of external stimuli as electric field (E) and magnetic field (H), the plot showed a power-law relationship of $\tau_y \propto E^{\alpha}$ [32] and $\tau_y \propto H^{\alpha}$ [28], respectively. The power-law index α was suggested to be 1.5 in conduction model and 2.0 in polarization model. The dependency of α of Fe_3O_4@PANI suspension was found to 1.5 for ER and 2.0 for MR system.

Some studies have defined an ER efficiency as $(\eta_E - \eta_0)/\eta_0$, where η_E is the viscosity in the presence of electric fields and η_0 is a zero electric field viscosity [13, 33]. In Figure 7, the efficiency increased with increasing electric field from 35 (0.5 kV/mm) to 484 (2.5 kV/mm) at 0.1 s^{-1}. On the other hand, at a high shear rate region, the efficiency decreased due to the destroyed gap-spanning particle chains resulting in weak resistance to flow [33]. At the low shear rate region, the ER efficiency is significantly higher with increasing electric field due to the high low shear viscosity. Similar to the ER efficiency, the ratio of the shear viscosity with and without a magnetic field can be considered an important factor for evaluating the MR efficiency. The efficiency increased more than 15 fold with increasing magnetic field strength from 15 (51 kA/m) to 227 (342 kA/m) at 0.1 s^{-1}. Consequently, Fe_3O_4@PANI suspension possessed the highest efficiency when 2.5 kV/mm was applied. Compared to other group's results dealing with ER or MR, it has higher ER efficiency than bare titania and GO-wrapped titania microspeheres [33], and lower than PANI/TiO_2 nanotubes [34]. Also, it is higher than spherical PANI/VO_2 and lower than flower-like PANI/VO_2 structures [35]. Poly(p-phenylenediamine) particles carbonized under 200°C [36] and PANI-coated carbonized PANI base [37] showed higher ER efficiency value. Nonetheless, the MR efficiency is lower than core-shell urchin-like ZnO coated carbonyl iron microparticles [10].

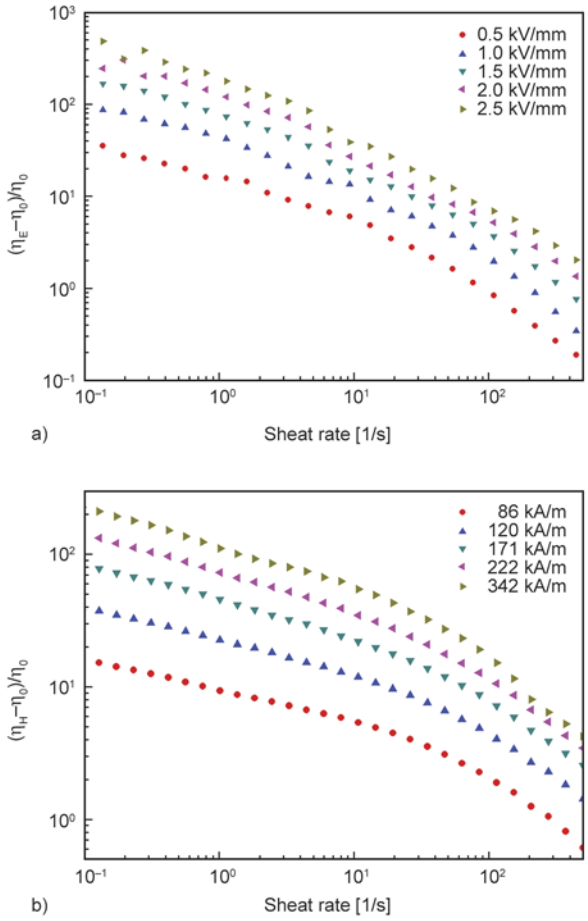

Figure 7. EMR efficiency of 20 wt% Fe_3O_4@PANI suspension under a) electric and b) magnetic fields

The dispersion stability of both Fe_3O_4 and Fe_3O_4@PANI suspension was examined using a Turbiscan, as shown in Figure 8. It measures the degree of light transmission as a function of time along the y-axis sample coordinates. Fe_3O_4@PANI stays steady compared to pure Fe_3O_4 more than five times. The sedimentation test corresponded to the decrease in particle density from 4.46 g/cm^3 (Fe_3O_4) to 2.76 g/cm^3 (Fe_3O_4@PANI) because the coating of polymer resulted in low density and can improve the dispersion stability.

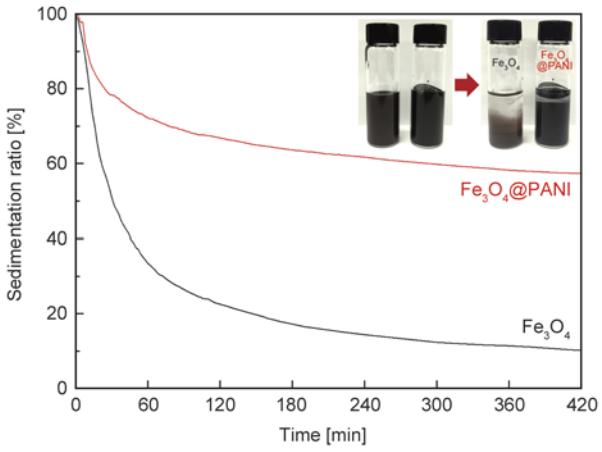

Figure 8. Sedimentation ratio of Fe_3O_4 and Fe_3O_4@PANI suspension (Inset: optical images of samples)

4. Conclusions

PANI-coated Fe_3O_4 was successfully prepared by solvothermal and oxidation polymerization. The chemical bond formation between Fe_3O_4 and PANI was confirmed by FT-IR spectroscopy, which showed a blue-shift and red-shift of PANI and Fe_3O_4 peaks, respectively. SEM and TEM images confirmed that PANI was attached well to the Fe_3O_4 surface. VSM data showed that magnetization saturation was 38 emu/g for Fe_3O_4@PANI which is lower than that of pure Fe_3O_4 particles. The prepared Fe_3O_4@PANI-based EMR suspension demonstrated typical ER or MR characteristics when electric or magnetic fields were applied, respectively, because of the conducting PANI-shell and magnetic Fe_3O_4-core structure. It is noteworthy that the suspension responded both of electric and magnetic fields and its sedimentation stability was also improved simultaneously.

Acknowledgements

This study was supported by Ministry of Trade, Industry and Energy, Korea through Daeheung RNT (# 10047791).

References

[1] Yao Z. L., Grishkewich N., Tam K. C.: Swelling and shear viscosity of stimuli-responsive colloidal systems. Soft Matter, **9**, 5319–5335 (2013). DOI: 10.1039/C3SM50374G

[2] Han M. S., Zhang X. Y., Li L., Peng C., Bao L., Ou E. C., Xiong Y. Q., Xu W. J.: Dual-switchable surfaces between hydrophobic and superhydrophobic fabricated by the combination of click chemistry and RAFT. Express Polymer Letters, **8**, 528–542 (2014). DOI: 10.3144/expresspolymlett.2014.56

[3] Thakur S., Karak N.: Multi-stimuli responsive smart elastomeric hyperbranched polyurethane/reduced graphene oxide nanocomposites. Journal of Materials Chemistry A, **2**, 14867–14875 (2014). DOI: 10.1039/C4TA02497D

[4] Fameau A-L., Saint-Jalmes A.: Yielding and flow of solutions of thermoresponsive surfactant tubes: Tuning macroscopic rheology by supramolecular assemblies. Soft Matter, **10**, 3622–3632 (2014). DOI: 10.1039/C3SM53001A

[5] Ahn S., Lee S. J.: Nanoparticle role on the repeatability of stimuli-responsive nanocomposites. Scientific Reports, **4**, 6624/1–6624/9 (2014). DOI: 10.1038/srep06624

[6] Zhang W. L., Choi H. J.: Stimuli-responsive polymers and colloids under electric and magnetic fields. Polymers, **6**, 2803–2818 (2014).
DOI: 10.3390/polym6112803

[7] Bica I., Anitas E. M., Bunoiu M., Vatzulik B., Juganaru I.: Hybrid magnetorheological elastomer: Influence of magnetic field and compression pressure on its electrical conductivity. Journal of Industrial and Engineering Chemistry, **20**, 3994–3999 (2014).
DOI: 10.1016/j.jiec.2013.12.102

[8] Bica I., Liu Y. D., Choi H. J.: Physical characteristics of magnetorheological suspensions and their applications. Journal of Industrial and Engineering Chemistry, **19**, 394–406 (2013).
DOI: 10.1016/j.jiec.2012.10.008

[9] Zhang X., Li W., Gong X.: Thixotropy of MR shear-thickening fluids. Smart Materials and Structures, **19**, 125012/1–125012/6 (2010).
DOI: 10.1088/0964-1726/19/12/125012

[10] Machovsky M., Mrlik M., Kuritka I., Pavlinek V., Babayan V.: Novel synthesis of core–shell urchin-like ZnO coated carbonyl iron microparticles and their magnetorheological activity. RSC Advances, **4**, 996–1003 (2014).
DOI: 10.1039/c3ra44982c

[11] Marins J. A., Soares B. G., Silva A. A., Hurtado M. G., Livi S.: Electrorheological and dielectric behavior of new ionic liquid/silica systems. Journal of Colloid and Interface Science, **405**, 64–70 (2013).
DOI: 10.1016/j.jcis.2013.05.013

[12] Mrlik M., Ilcikova M., Sedlacik M., Mosnacek J., Peer P., Filip P.: Cholesteryl-coated carbonyl iron particles with improved anti-corrosion stability and their viscoelastic behaviour under magnetic field. Colloid and Polymer Science, **292**, 2137–2143 (2014).
DOI: 10.1007/s00396-014-3245-5

[13] Lengálová A., Pavlínek V., Sáha P., Quadrat O., Kitano T., Stejskal J.: Influence of particle concentration on the electrorheological efficiency of polyaniline suspensions. European Polymer Journal, **39**, 641–645 (2003).
DOI: 10.1016/S0014-3057(02)00281-1

[14] Wang B., Yin Y., Liu C., Yu S., Chen K.: Synthesis of flower-like $BaTiO_3/Fe_3O_4$ hierarchically structured particles and their electrorheological and magnetic properties. Dalton Transactions, **42**, 10042–10055 (2013).
DOI: 10.1039/c3dt50504a

[15] Jang W. H., Kim J. W., Choi H. J., Jhon M. S.: Synthesis and electrorheology of camphorsulfonic acid doped polyaniline suspensions. Colloid and Polymer Science, **279**, 823–827 (2001).
DOI: 10.1007/s003960100534

[16] Fang F. F., Liu Y. D., Choi H. J.: Electrorheological and magnetorheological response of polypyrrole/magnetite nanocomposite particles. Colloid and Polymer Science, **291**, 1781–1786 (2013).
DOI: 10.1007/s00396-013-2913-1

[17] Bednarek S.: Electromagnetorheological suspensions and inducted changes of their magnetic permeability and dielectric constant. Review of Scientific Instruments, **70**, 1505–1510 (1999).
DOI: 10.1063/1.1149614

[18] Minagawa K., Watanabe T., Koyama K., Sasaki M.: Significant synergistic effect of superimposed electric and magnetic fields on the rheology of iron suspension. Langmuir, **10**, 3926–3928 (1994).
DOI: 10.1021/la00023a003

[19] Korobko E. V., Novikova Z. A., Zhurauski M. A., Borin D., Odenbach S.: Synergistic effect in magnetoelectrorheological fluids with a complex dispersed phase. Journal of Intelligent Material Systems and Structures, **23**, 963–967 (2012).
DOI: 10.1177/1045389X11429174

[20] Han X., Gai L., Jiang H., Zhao L., Liu H., Zhang W.: Core–shell structured Fe_3O_4/PANI microspheres and their Cr(VI) ion removal properties. Synthetic Metals, **171**, 1–6 (2013).
DOI: 10.1016/j.synthmet.2013.02.025

[21] Zheng W., Angelopoulos M., Epstein A. J., MacDiarmid A. G.: Experimental evidence for hydrogen bonding in polyaniline: Mechanism of aggregate formation and dependency on oxidation state. Macromolecules, **30**, 2953–2955 (1997).
DOI: 10.1021/ma9700136

[22] Liu W., Kumar J., Tripathy S., Samuelson L. A.: Enzymatic synthesis of conducting polyaniline in micelle solutions. Langmuir, **18**, 9696–9704 (2002).
DOI: 10.1021/la0206357

[23] Zheng Y-H., Cheng Y., Bao F., Wang Y-S.: Synthesis and magnetic properties of Fe_3O_4 nanoparticles. Materials Research Bulletin, **41**, 525–529 (2006).
DOI: 10.1016/j.materresbull.2005.09.015

[24] Gai L., Du G., Zuo Z., Wang Y., Liu D., Liu H.: Controlled synthesis of hydrogen titanate–polyaniline composite nanowires and their resistance–temperature characteristics. The Journal of Physical Chemistry C, **113**, 7610–7615 (2009).
DOI: 10.1021/jp900369y

[25] Deng J., He C., Peng Y., Wang J., Long X., Li P., Chan A. S. C.: Magnetic and conductive Fe_3O_4–polyaniline nanoparticles with core–shell structure. Synthetic Metals, **139**, 295–301 (2003).
DOI: 10.1016/S0379-6779(03)00166-8

[26] Cho M. S., Cho Y. H., Choi H. J., Jhon M. S.: Synthesis and electrorheological characteristics of polyaniline-coated poly(methyl methacrylate) microsphere: Size effect. Langmuir, **19**, 5875–5881 (2003).
DOI: 10.1021/la026969d

[27] Stěnička M., Pavlínek V., Sáha P., Blinova N. V., Stejskal J., Quadrat O.: The electrorheological efficiency of polyaniline particles with various conductivities suspended in silicone oil. Colloid and Polymer Science, **287**, 403–412 (2009).
DOI: 10.1007/s00396-008-1977-9

[28] Bossis G., Lacis S., Meunier A., Volkova O.: Magnetorheological fluids. Journal of Magnetism and Magnetic Materials, **252**, 224–228 (2002).
DOI: 10.1016/S0304-8853(02)00680-7

[29] Jang I. B., Kim H. B., Lee J. Y., You J. L., Choi H. J., Jhon M. S.: Role of organic coating on carbonyl iron suspended particles in magnetorheological fluids. Journal of Applied Physics, **97**, 10Q912/1–10Q912/3 (2005).
DOI: 10.1063/1.1853835

[30] Orihara H., Nishimoto Y., Aida K., Na Y. H., Nagaya T., Ujiie S.: Morphology and rheology of an immiscible polymer blend subjected to a step electric field under shear flow. Journal of Physics: Condensed Matter, **23**, 284106/1–284106/6 (2011).
DOI: 10.1088/0953-8984/23/28/284106

[31] Park B. J., Hong M. K., Choi H. J.: Atom transfer radical polymerized PMMA/magnetite nanocomposites and their magnetorheology. Colloid and Polymer Science, **287**, 501–504 (2009).
DOI: 10.1007/s00396-009-2013-4

[32] Klingenberg D. J., van Swol F., Zukoski C. F.: The small shear rate response of electrorheological suspensions. II. Extension beyond the point–dipole limit. The Journal of Chemical Physics, **94**, 6170–6178 (1991).
DOI: 10.1063/1.460403

[33] Yin J., Shiu Y., Dong Y., Zhao X.: Enhanced dielectric polarization and electro-responsive characteristic of graphene oxide-wrapped titania microspheres. Nanotechnology, **25**, 045702/1–045702/11 (2014).
DOI: 10.1088/0957-4484/25/4/045702

[34] Cheng Q., Pavlinek V., He Y., Li C., Saha P.: Electrorheological characteristics of polyaniline/titanate composite nanotube suspensions. Colloid and Polymer Science, **287**, 435–441 (2009).
DOI: 10.1007/s00396-008-1985-9

[35] Goswami S., Brehm T., Filonovich S., Cidade M. T.: Electrorheological properties of polyaniline-vanadium oxide nanostructures suspended in silicone oil. Smart Materials and Structures, **23**, 105012/1–105012/10 (2014).
DOI: 10.1088/0964-1726/23/10/105012

[36] Plachy T., Sedlacik M., Pavlinek V., Morávková Z. Hajná M., Stejskal J.: An effect of carbonization on the electrorheology of poly(*p*-phenylenediamine). Carbon, **63**, 187–195 (2013).
DOI: 10.1016/j.carbon.2013.06.070

[37] Sedlacik M., Pavlinek V., Mrlik M., Morávková Z., Hajná M., Trchová M., Stekskal J.: Electrorheology of polyaniline, carbonized polyaniline, and their core–shell composites. Materials Letters, **101**, 90–92 (2013).
DOI: 10.1016/j.matlet.2013.03.084